Journal of ELECTRICAL ENGINEERING, VOL 66. NO 7/s, 2015, 82-85

MAGNETOELASTIC PROPERTIES OF $X_{30}Cr_{13}$ CONSTRUCTIONAL STEEL IN RAYLEIGH REGION

Maciej Kachniarz* – Roman Szewczyk**

In the paper results of the investigation of magnetoelastic properties of X30Cr13 constructional steel in Rayleigh region are presented. Digitally controlled measurement setup utilizing hydraulic press for applying mechanical stresses is described and methodology of measuring magnetic hysteresis loop in Rayleigh region is discussed. On the basis of the obtained magnetoelastic characteristics, mathematical model of the investigated phenomenon is determined, including polynomial equations describing changes of initial magnetic permeability and so called Rayleigh coefficient depending on the value of applied mechanical stress, which allows to simulate shape of the Rayleigh hysteresis loop under given value of mechanical stress. Obtained modeling results show high compatibility with experimental data, which indicates that determined model can be used to simulate influence of mechanical stress on the magnetic properties X30Cr13 constructional steel in Rayleigh region. This allows to suppose that similar models can be developed for other constructional ferromagnetic materials.

Keywords: magnetoelastic effect, Rayleigh region, constructional steel, modelling

1 INTRODUCTION

Steel is one of the most commonly utilized constructional materials. This creates a great need for methods of monitoring the state of the steel material working under stresses, mostly for safety reasons. This need can be fulfilled by using non-destructive testing (NDT) methodology based on magnetoelastic Villari reversal effect [1]. The major obstacle in application of this method in industrial conditions is lack of knowledge about magnetoelastic properties of constructional ferromagnetic materials like steel, especially in low magnetizing fields.

Rayleigh region is the first part of the initial magnetization curve, where ferromagnetic material is subjected to the low magnetizing fields [2]. Due to low, easy to obtain magnetizing fields, Rayleigh region seems to be very interesting from the point of view of non-destructive testing methods based on magnetoelastic effect [3, 4].

2 THEORY OF RAYLEIGH REGION

Term Rayleigh region refers to the first part of the initial magnetization curve, where magnetizing filed acting on the material is relatively low [2]. For each material the range of magnetizing field's values considered as Rayleigh region is different, depending on its ferromagnetic properties, especially coercive field H_c. In this region, initial magnetization curve is described by second order equation with two material parameters: initial relative permeability μ_i and Rayleigh coefficient α_R [2]:

$$B(H) = \mu_0 \mu_i H + \mu_0 \alpha_R H^2 \tag{1}$$

where B is magnetic flux density, H is magnetizing field and μ_0 is vacuum magnetic permeability. Presented equation is known as Rayleigh law and describes the first, parabolic part of the initial magnetization curve [2]. Linear part of the equation (1) is connected with reversible magnetization process occurring due to elastic deflections of the Bloch domain walls. The second order part of Rayleigh law describes irreversible magnetization resulting from translations of the Bloch domain walls caused by imperfections in the crystalline structure of the material [5]. The irreversible magnetization process results in occurrence of magnetic hysteresis phenomenon in Rayleigh region. Unlike in near-saturation region, hysteresis loop in Rayleigh region (Rayleigh hysteresis loop) has lenticular shape, as it is composed of two parabolic curves of which one is upper, decreasing branch of the loop given with the equation:

$$B(H) = \mu_0[(\mu_i + \alpha_R H_m)H + \frac{\alpha_R}{2}(H_m^2 - H^2)] \tag{2}$$

where H_m is amplitude of the magnetizing field, and the second one is lower, increasing branch:

$$B(H) = \mu_0[(\mu_i + \alpha_R H_m)H - \frac{\alpha_R}{2}(H_m^2 - H^2)] \tag{3}$$

The intersection points of this two parabolic curves are the vertices of the Rayleigh hysteresis loop.

As it was previously reported, magnetoelastic Villari effect is also observable in Rayleigh region [6], which creates a possibility to utilize this phenomenon in NDT method of stress assessment in steel constructions. Important aspect of studies on the Villari reversal effect in Rayleigh region is also modelling of the magnetomechanical properties of ferromagnetic materials. Most of models developed so far is focused on high magnetizing fields in near saturation region [7-9]. Jiles-Atherton model, expanded with the influence of magnetomechanical effect was adapted for the Rayleigh region [10], but obtained results exhibited significant differences from experimental data. In this paper much simpler model is presented, based on polynomial equations describing mechanical stress dependence of material parameters in equation (1).

* Industrial Research Institute for Automation and Measurements, al. Jerozolimskie 202, 02-486 Warsaw, Poland; mkachniarz@piap.pl, ** Institute of Metrology and Biomedical Engineering, Warsaw University of Technology, sw. Andrzeja Boboli 8, 05-525 Warsaw, Poland; r.szewczyk@mchtr.pw.edu.pl

ISSN 1335-3632

3 EXPERIMENTAL SETUP

For performed experiment, special frame-shaped samples of investigated X30Cr13 steel and digitally controlled measurement system were developed allowing to measure magnetic parameters of the material under mechanical stress.

3.1 Investigated material

The investigated material was X30Cr13 ferromagnetic constructional steel utilized mostly in energetic industry as material for turbines elements. It is martensitic corrosion resistant alloy steel with addition of chromium (about 12-14%) [11].

For the experiment, investigated material was formed in special frame-shaped sample, presented in Fig. 1. This shape allowed to obtain closed magnetic circuit in the material (reduction of the influence of demagnetizing field) as well as nearly uniform distribution of applied mechanical stress in the sample.

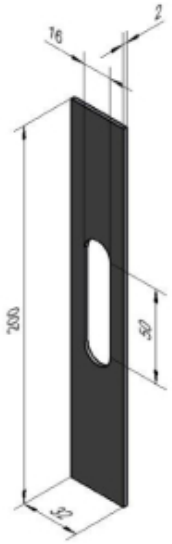

Fig. 1. Frame-shaped sample designed for the experiment

In order to measure magnetic characteristics of the material, on the columns of the sample two sets of windings were made: 40 turns of magnetizing winding and 200 turns of sensing winding. Relatively large number of sensing winding results from low values of magnetic flux density in Rayleigh region. Both sets of windings were made on non-magnetic pads protecting the wire form breaking while sample changes its dimensions under the influence of applied mechanical stress.

3.2 Measurement system

For the investigation special measurement stand was developed composed of digitally controlled system for magnetic materials investigation HB-PL30 and stress generation setup. Schematic block diagram of the measurement system is presented in Fig. 2.

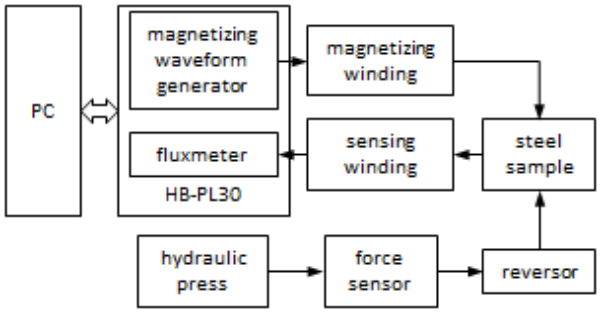

Fig. 2. Schematic block diagram of the measurement system

HB-PL30 system contains magnetizing waveform generator composed of sinusoidal voltage waveform generator and voltage to current converter. Generated magnetizing waveform is applied to the magnetizing winding of the investigated sample. Changes of the magnetizing field results in changes of the voltage induced in the sensing winding, which is measured by the fluxmeter built into HB-PL30 system. The system is controlled by the PC, which also acquires and processes measurement data.

Oil hydraulic press is used to generate mechanical stress in the investigated sample. To convert compressive force applied with the press to tensile force acting on the sample, special force reversor was designed, presented in Fig. 3. Value of the force applied with the press is measured by the precise for sensor and then converted into value of applied tensile stress.

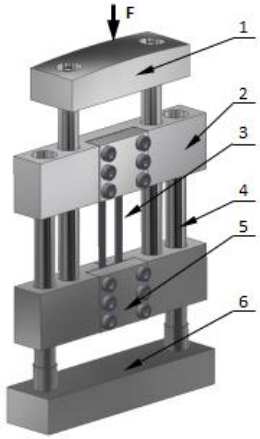

Fig. 3. Force reversor used in the experiment: 1 – upper bar, 2 – moving bar, 3 – frame-shaped sample, 4 – cylindrical column, 5 – sample holder, 6 – reversor base

4 EXPERIMENTAL RESULTS AND MODELLING

During the investigation frame-shaped sample of X30Cr13 steel was subjected to the tensile stress σ_T in the range from 0 to 575 MPa, where sample started to break. For each value of the applied stress hysteresis loops were measured for amplitude of magnetizing field H_m from 50 A/m to 450 A/m, which corresponds to the Rayleigh region for investigated steel. As a result, family

of Rayleigh hysteresis loops depending on the value of σ_T for each value of H_m was obtained. Exemplary family of selected Rayleigh hysteresis loops for H_m = 450 A/m is presented in Fig. 4.

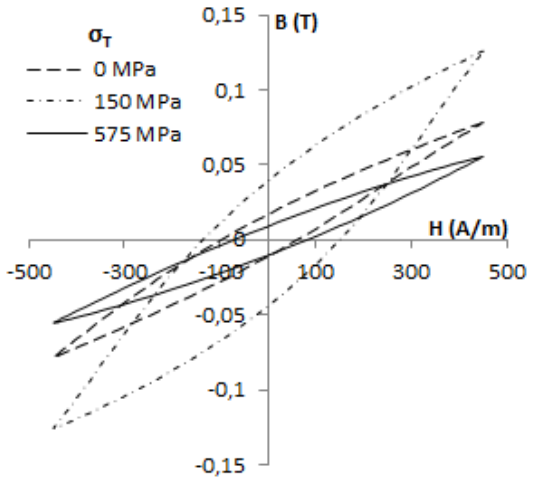

Fig. 4. Family of selected Rayleigh hysteresis loops of X30Cr13 constructional steel for H_m = 450 A/m

For all values of applied tensile stress σ_T, Rayleigh hysteresis loops maintain their lenticular shape. For initial values of σ_T, from 0 to 150 MPa, surface area of Rayleigh hysteresis loop is growing, as well as basic magnetic parameters: maximum magnetic flux density B_m, coercive field H_c and remanence B_r. After σ_T = 150 MPa, which is Villari reversal point for X30Cr13 steel, surface of the loop and values of B_m, H_c, and B_r are constantly decreasing up to rupture point σ_T = 575 MPa.

Figure 5 presents selected magnetoelastic characteristics $B_m(\sigma_T)$ for investigated steel. As it can be seen, Villari reversal point at σ_T = 150 MPa is clearly observable.

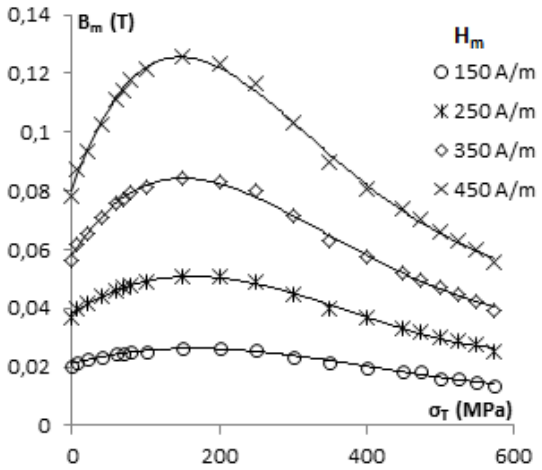

Fig. 5. Selected magnetoelastic characteristics $B_m(\sigma_T)$ of X30Cr13 constructional steel

On the basis of the obtained results, $B_m(H_m)$ characteristics for all values of applied tensile stress σ_T were designated. For each value of σ_T, $B_m(H_m)$ characteristic was fitted with second order polynomial equation of general form

$$B_m = aH_m^{\,2} + bH_m + c \tag{4}$$

where a, b and c are coefficients of the equation. Comparing obtained equations with equation (1) allowed calculating values of the Rayleigh coefficient α_R and initial relative permeability μ_i for each value of applied compressive stress σ_T:

$$\alpha_R = \frac{a}{\mu_0} \tag{5}$$

$$\mu_i = \frac{b}{\mu_0} \tag{6}$$

As a result of this operation, characteristics of α_R and μ_i depending on the value of tensile stress σ_T were obtained, which are presented in Fig. 6 and Fig. 7.

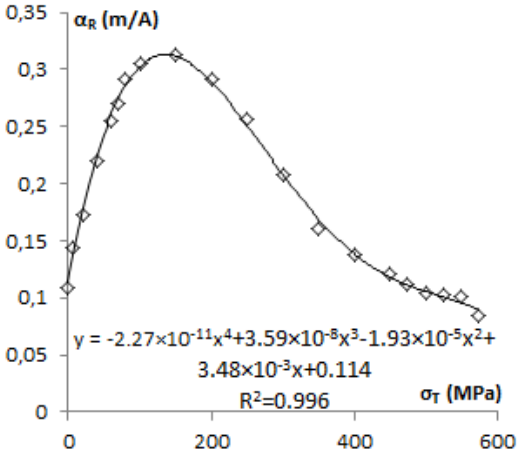

Fig. 6. The tensile stress σ_T dependence of Rayleigh coefficient α_R for of X30Cr13 constructional steel

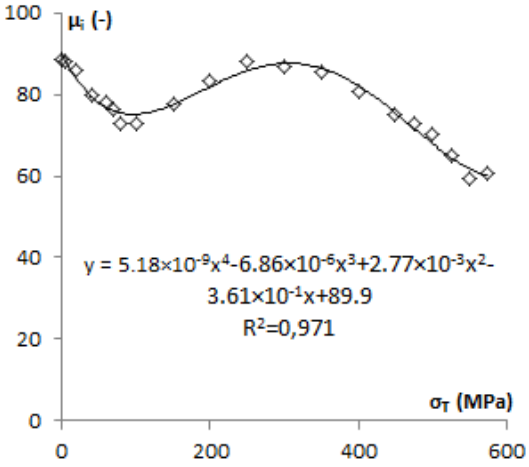

Fig. 7. The tensile stress σ_T dependence of initial permeability μ_i for of X30Cr13 constructional steel

Both resultant characteristics were fitted with polynomial curves of fourth order, which ensured high value of determination coefficient R^2, which is 0.996 for α_R and 0.971 for μ_i. As a result, system of two equations describ-

ing changes of material parameters under the influence of tensile stress σ_T was obtained:

$$\alpha_R(\sigma_T) = -2.27\times10^{-11}\sigma_T^4 + 3.59\times10^{-8}\sigma_T^3 - 1.93\times10^{-5}\sigma_T^2 + 3.48\times10^{-3}\sigma_T + 0.114 \quad (7)$$

$$\mu_i(\sigma_T) = 5.18\times10^{-9}\sigma_T^4 - 6.86\times10^{-6}\sigma_T^3 + 2.77\times10^{-3}\sigma_T^2 - 3.61\times10^{-1}\sigma_T + 89.9 \quad (8)$$

Obtained equations allow to determine values of material parameters α_R and μ_i for given value of tensile stress σ_T from the range 0 – 575 MPa. When values calculated from the equations (7) and (8) are substituted to the equations (2) and (3), it is possible to model shape of the Rayleigh hysteresis loop for given value of σ_T in the material.

In order to validate correctness of the presented model, the results of modelling were compared with measurement data for three validation points of σ_T value. In every point of σ_T results were compared for three values of amplitude of magnetizing field H_m. The measured data were the result of investigation of identical sample of X30Cr13 steel treated as a validation one. The exemplary result of validation is presented in Fig. 8.

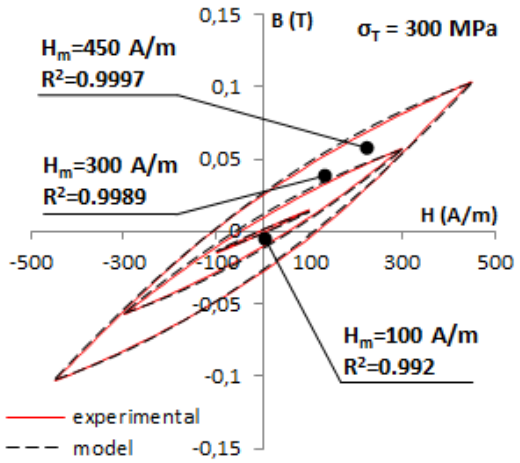

Fig. 8. Results of validation of presented model for tensile stress σ_T = 300 MPa

For each validation point determination coefficient R^2 was calculated for all three Rayleigh hysteresis loops (at three values of H_m). The results are presented in Table 1.

Table 1. Values of determination coefficient R^2 in validation points

Determination coefficient R^2

H_m(A/m) \ σ_T (MPa)	60	300	575
100	0.974	0.992	0.998
300	0.998	0.9989	0.9996
450	0.9989	0.9997	0.9991

As it can be seen, obtained values of determination coefficient R^2 are close to 1 (the least value is 0,974), which indicates that presented model is correct and there is strong correlation between modelling results and experimental data.

5 CONCLUSION

Presented magnetoelastic characteristics of X30Cr13 constructional steel show significant correlation between applied tensile stress and magnetic properties of the material. For the first time stress dependence of Rayleigh coefficient and initial relative permeability of constructional steel were determined.

As a result of performed measurements and calculations, simplified model for technical applications describing magnetoelastic properties of X30Cr13 steel in Rayleigh region was obtained. Presented model is characterized by high compatibility between results of modelling and experimental data. It is also very simple and can be easily utilized in technical applications, especially in magnetoelastic-based methodology of non-destructive testing.

However, presented model is only simplified technical description. Full understanding of the discussed phenomenon requires further works involving development of more complex physical model taking into account processes occurring in the domain structure of the material subjected to mechanical stress.

REFERENCES

[1] BIEŃKOWSKI, A.: Magnetoelastic Villari effect in Mn-Zn ferrites, J. Magn. Magn. Mater. **215-216** (2000), 231-233
[2] JILES, D.C.: Introduction to Magnetism and Magnetic Materials 2nd ed., CHAPMAN&HALL, London (1998)
[3] SHI, Y. – FAN, S.: Application of Magnetoelastic Effect of Ferromagnetic Material in Stress Measurement, Adv. Mat. Res. **496** (2012), 306-309
[4] JACKIEWICZ, D. – KACHNIARZ, M. – ROZNIATOWSKI, K. *et al*.: Temperature Resistance of Magnetoelastic Characteristics of 13CrMo4-5 Constructional Steel, Acta. Phys. Pol. A **127** (2015), 614-616
[5] NOVÁK, L. – KOVÁČ , J.: Rayleigh Region in Amorphous and Nanocrystaline FINEMET Alloy, Acta. Phys. Pol. A **126** (2014), 126-127
[6] BIRSS, R.R.: Magnetomechanical Effects in the Rayleigh Region, IEEE Trans. Magn. **MAG-7** (1971), 113-133
[7] LIORZOU, F. – PHELPS, B. – ATHERTON, D.L.: Macroscopic Models of Magnetization, IEEE Trans. Magn. **36** (2000), 418-428
[8] SZEWCZYK, R. – BIENKOWSKI, A. – SALACH, J.: Extended Jiles-Atherton model for modelling the magnetic characteristics of isotropic materials, J. Magn. Magn. Mater. **320** (2008), 1049-1052
[9] JACKIEWICZ, D. – SZEWCZYK, R. – SALACH, J. – BIENKOWSKI, A.: Application of Extended Jiles-Atherton Model for Modelling the Influence of Stresses on Magnetic Characteristics of the Construction Steel, Acta. Phys. Pol. A **126** (2016), 392-393
[10] LI, L. – JILES, D.C.: Modified Law of Approach for the Magnetomechanical Model: Application of the Rayleigh Law to Stress, IEEE Tarns. Magn. **39** (2003), 3037-3039
[11] EN 10088-1:2005 Stainless steels. List of stainless steels

Received 30 November 2015